Binding of Amyloidogenic Transthyretin to the Plasma Membrane Alters Membrane Fluidity and Induces Neurotoxicity †

ARTICLE *in* BIOCHEMISTRY · AUGUST 2005

Impact Factor: 3.02 · DOI: 10.1021/bi050700m · Source: PubMed

4 AUTHORS, INCLUDING:

Samantha J Richardson
RMIT University
85 PUBLICATIONS **1,808** CITATIONS
SEE PROFILE

Marie-Isabel Aguilar
Monash University (Australia)
222 PUBLICATIONS **4,644** CITATIONS
SEE PROFILE

David H Small
University of Tasmania
179 PUBLICATIONS **6,547** CITATIONS
SEE PROFILE

Binding of Amyloidogenic Transthyretin to the Plasma Membrane Alters Membrane Fluidity and Induces Neurotoxicity†

Xu Hou,‡ Samantha J. Richardson,§ Marie-Isabel Aguilar,‡ and David H. Small*,‡

Department of Biochemistry and Molecular Biology, Monash University, Clayton, VIC 3800, Australia, and Department of Biochemistry and Molecular Biology, University of Melbourne, Parkville, VIC 3010, Australia

Received April 17, 2005; Revised Manuscript Received May 31, 2005

ABSTRACT: Transthyretin (TTR) can deposit as amyloid in the peripheral nervous system and induce a peripheral neuropathy. We examined the mechanism of TTR amyloid neurotoxicity on SH-SY5Y neuroblastoma cells. Wild-type (WT) TTR and two amyloidogenic mutants (V30M and L55P) were expressed in *Escherichia coli*. Incubation (aging) of WT TTR at 37 °C for 1 week caused no significant aggregation. However, there was a significant increase in the extent of amyloid fibril formation after the amyloidogenic mutants had been aged. L55P TTR aggregated more readily than V30M TTR. Both amyloidogenic mutants were neurotoxic after aging. The order of neurotoxicity was as follows: L55P > V30M > WT. As binding of amyloid proteins to the plasma membrane may cause cytotoxicity, we studied the binding of TTR to a plasma membrane-enriched preparation from SH-SY5Y cells by surface plasmon resonance. All three forms bound to the plasma membrane through electrostatic interactions. The binding of the amyloidogenic mutants was increased by aging. The amount of binding correlated closely with the amount of aggregation and with the cytotoxicity of each form. As membrane fluidity can influence cell viability, we also examined the effect of TTR on membrane fluidity using a fluorescence anisotropy method. Binding of the amyloidogenic TTR mutants increased membrane fluidity, and once again, the order of potency was as follows: L55P > V30M > WT. These results demonstrate that TTR can bind to the plasma membrane and cause a change in membrane fluidity. Altered membrane fluidity may be the cause of the neurotoxicity.

A number of neurodegenerative diseases are caused by the aggregation and deposition of amyloid in the nervous system (*1*). For example, the deposition of β-amyloid peptide (Aβ)[1] is considered to be a key event in the pathogenesis of Alzheimer's disease, which is the prototypic amyloidosis (*2*). However, the mechanism by which amyloidogenic proteins cause neurotoxicity is unclear (*3*).

Transthyretin (TTR) is a plasma protein produced in the liver and the choroid plexus that can form amyloid (*4*, *5*). TTR is the predominant component of the amyloid fibrils in familial amyloidotic polyneuropathy (FAP), a hereditary disorder characterized by systemic extracellular deposition of amyloid fibrils, mainly in the peripheral nervous system (*6*, *7*). Native TTR consists of four identical subunits that form an extensive β-sheet structure, which is prone to misfolding upon mutation (*8*, *9*). So far, nearly 80 mutations have been identified in TTR, most of which are amyloidogenic (*10*). It is believed that structural modifications by these mutations destabilize the native tetrameric conformation and favor its dissociation into monomeric structure, which is the building block of TTR amyloid fibrils (*11*, *12*). Incubation of amyloidogenic TTR over several days at 37 °C, a process known as "aging", increases the amount of TTR amyloid and also increases the cytotoxicity of TTR (*13*).

Although a few hypotheses have been proposed for the pathogenesis of neurodegeneration in FAP (*5*, *14*), the molecular basis of TTR amyloid cytotoxicity is yet to be elucidated. It has been suggested that the cytotoxicity of amyloids (e.g., Aβ) is a direct consequence of binding to the plasma membrane (*15*, *16*). Therefore, in this study, we have examined whether TTR can bind to the plasma membrane and whether this binding could explain the toxic effects of TTR seen in cell culture.

To study binding of TTR to the plasma membrane, we used the surface plasmon resonance (SPR) biosensor technique, which has previously been used for the study of Aβ−membrane interactions (*17*, *18*). We show here that TTR binds to the lipids of the plasma membrane through electrostatic interactions and that the amount of binding is increased upon TTR aggregation. We also show that the amount of TTR binding to the plasma membrane correlates with the degree of cytotoxicity observed in cell culture.

† This work was supported by the National Health and Medical Research Council (NHMRC) of Australia and a sponsored research agreement with Axonyx Inc. (New York, NY).

* To whom correspondence should be addressed: Department of Biochemistry and Molecular Biology, Monash University, Clayton, VIC 3800, Australia. Telephone: 61-3-9905 3743. Fax: 61-3-9905 3726. E-mail: David.Small@med.monash.edu.au.

‡ Monash University.

§ University of Melbourne.

[1] Abbreviations: TTR, transthyretin; SPR, surface plasmon resonance; FAP, familial amyloidotic polyneuropathy; Aβ, β-amyloid protein; IPTG, isopropyl β-D-thiogalactopyranoside; LDH, lactate dehydrogenase; DMPC, dimyristoyl-L-α-phosphatidylcholine; DMPS, dimyristoyl-L-α-phosphatidylserine; DMPE, dimyristoyl-L-α-phosphatidylethanolamine; SM, sphingomyelin; CL, cholesterol; RU, response units; DPH, 1,6-diphenyl-1,3,5-hexatriene; PrP, prion protein.

10.1021/bi050700m CCC: $30.25
Published on Web 08/05/2005

Finally, we demonstrate that binding of TTR amyloid to the plasma membrane alters membrane fluidity, providing a possible explanation for the cytotoxic effect.

EXPERIMENTAL PROCEDURES

Expression and Purification of TTR. Plasmids (pMMHA) containing two amyloidogenic TTR mutants, V30M and L55P, and wild-type (WT) TTR were the generous gift of J. W. Kelly (The Scripps Research Institute, La Jolla, CA). In each case, the cDNA sequence was cloned after the T7 promoter between the *Pst*I and *Bam*HI sites. The plasmids were transformed into the competent cells of BL21(DE3)-RIG CodonPlus *Escherichia coli* (kindly provided by S. Easterbrook-Smith, School of Molecular and Microbial Biosciences, The University of Sydney, Sydney, Australia). Heterologous expression was induced by the addition of 1.75 mM IPTG at an A_{600} of 0.6−0.7. The cells were harvested 4 h after induction by centrifugation and resuspended in 50 mM Tris-HCl (pH 8.0). The cells were disrupted with a Branson Sonifier 450 sonicator (Branson Sonic Power, Danbury, CT) at power level 5 and 50% duty for 20 bursts. After centrifugation, TTR was precipitated from the supernatant fraction at 50−90% saturated ammonium sulfate, and the resulting pellet was dissolved in 5 mL of 50 mM Tris-HCl (pH 8.0) and dialyzed against 5 L of the same buffer with four or five changes over 24 h. The dialyzed sample was then loaded onto an anion-exchange column (5 mL Econo-Pac Q cartridge, Bio-Rad, Hercules, CA) and eluted with a linear gradient from 0 to 0.5 M NaCl in 50 mM Tris-HCl (pH 8.0) over 40 min at 1.0 mL/min using a Biologic Workstation (Bio-Rad). The fraction of 0.15−0.25 M NaCl was collected, buffer exchanged, and concentrated in 20 mM phosphate buffer (pH 7.4) containing 150 mM NaCl by Centriplus YM-10 centrifugal filter units (Millipore, Billerica, MA). TTR was further purified by size-exclusion chromatography on an Agilent 1100 series HPLC system using a Zorbax GF-250 column (4.6 mm × 250 mm, Agilent Technologies), with 20 mM phosphate buffer (pH 7.4) containing 150 mM NaCl at a flow rate of 1.0 mL/min. The final purity of TTR was determined by SDS−PAGE and MALDI-MS to be >95%. Purified TTR was adjusted to a concentration of 100 μM (5.5 mg/mL) in 20 mM phosphate buffer (pH 7.4) containing 150 mM NaCl and stored at −80 °C.

Measurement of the Extent of TTR Aggregation. Stock solutions of V30M, L55P, and WT TTR were diluted in 20 mM phosphate buffer (pH 7.4) containing 150 mM NaCl to give a range of concentrations from 1 to 40 μM. The solutions were aged at 37 °C for 1 week. The extent of total aggregation was determined by changes in turbidity by monitoring the absorbance of the solution at 330 nm using a Bio-Rad SmartSpec 3000 spectrophotometer (*19*). Aggregation was also monitored by size-exclusion chromatography using a Zorbax GF-250 column (4.6 mm × 250 mm) on an Agilent 1100 series HPLC system. TTR was eluted with phosphate buffer (20 mM, pH 7.4) containing 150 mM NaCl at a flow rate of 1.0 mL/min and the eluate monitored by the absorbance at 280 nm. Finally, the concentration of TTR amyloid was determined using a Congo red binding assay following the procedures of Lai et al. (*19*). In this assay, the TTR solution (50 μL) was added to 1150 μL of 10 μM Congo red in 20 mM phosphate buffer (pH 7.4) containing 150 mM NaCl. The absorbance of the solution was measured at 477 and 540 nm using a Bio-Rad SmartSpec 3000 spectrophotometer after incubation at room temperature for 15 min. The concentration of TTR amyloid fibrils, represented by the moles of bound Congo red per liter of TTR solution, was determined by the formula (*19*)

$$[\text{TTR amyloid}] = A_{540}/25295 - A_{477}/46306$$

Cell Culture. Human SH-SY5Y neuroblastoma cells (from the Department of Pathology, University of Melbourne) were cultured in DMEM/F12 medium containing 50 units/mL penicillin and 50 μg/mL streptomycin, supplemented with 10% (v/v) fetal calf serum at 37 °C in a humidified atmosphere with 5% CO_2.

MTS Assay of Cell Viability. Cell viability was determined using the CellTiter 96 Aqueous One Solution Cell Proliferation Assay kit (Promega Corp.), which employs the MTS reagent [3-(4,5-dimethylthiazol-2-yl)-5-(3-carboxymethoxyphenyl)-2-(4-sulfophenyl)-2*H*-tetrazolium]. SH-SY5Y cells were plated in a 96-well plate at a density of $4-5 \times 10^3$ cells in 100 μL of medium per well. Serum-free DMEM/F12 medium containing 10 μM freshly prepared or aged TTR was used to replace the serum-supplemented medium after plating for 48 h. Cells incubated in serum-free medium without TTR were used as the control. MTS reagent (10%, v/v) was added to the cells after TTR treatment for 24 h, and then incubated at 37 °C for 2 h. The viability of the cells was measured by the absorbance at 490 nm using a Bio-Rad model 550 microplate reader. The cytotoxicity of TTR was calculated from the decrease in the amount of reduced MTS (A_{490}) compared to the control.

LDH Assay of Cell Death. An LDH assay was performed to determine the amount of cell death in the culture. SH-SY5Y cells were plated in a 96-well plate at a density of $5-6 \times 10^3$ cells in 150 μL of medium per well. The medium was replaced with serum-free DMEM/F12 medium containing 10 μM freshly prepared or aged TTR after plating for 48 h. Cells incubated in serum-free medium without TTR were used as the control. Following incubation at 37 °C for 24 h, the plate was centrifuged at 250*g* for 10 min and 100 μL of the supernatant fraction was transferred from each well to another plate. A cytotoxicity detection kit (LDH) (Roche Diagnostics Australia) was used, and the reaction mixture was made according to the instructions. The reaction mixture (100 μL) was added to 100 μL of medium. The absorbance at 490 nm was measured using a Bio-Rad model 550 microplate reader after incubation in darkness for 15 min at room temperature. The cytotoxicity of the TTR was calculated from the increase in the lactate dehydrogenase (LDH) activity (A_{490}) compared to the control.

Preparation of a Plasma Membrane-Enriched Fraction. A plasma membrane-enriched fraction from SH-SY5Y cells was prepared by using an aqueous two-phase polymer method (*20*). SH-SY5Y cells (7×10^8) were resuspended in 1 mM $NaHCO_3$ containing 0.2 mM EDTA at a density of 10^8 cells/mL, and gently shaken for 40 min to allow the cells to swell. The cells were lysed with a Dounce glass−glass homogenizer (Kontes, Vineland, NJ). The cell lysate was centrifuged twice at 1000*g* for 10 min in an Allegra 21R centrifuge using a Beckman S4180 rotor (Beckman Coulter, Fullerton, CA) to eliminate unbroken cells and nuclei. The

supernatant fraction containing microsomes and mitochondria was then centrifuged at 45000*g* for 30 min in an Optima L-90K ultracentrifuge using a SW 41Ti rotor (Beckman Coulter). The pellet was resuspended in 50 mM Tris-HCl (pH 8.0) to 8 g in weight. Four aliquots of the aqueous two-phase polymer mixture were made weighing 16 g each, containing 2 g of the resuspended pellet, 6.6% (w/w) Dextran T-500 (Amersham-Pharmacia), 6.6% (w/w) polyethylene glycol 3350 (Sigma), 0.25 M sucrose, and 5 mM potassium phosphate (pH 7.2). The contents of the two-phase system were mixed thoroughly at 4 °C for 40 min, and then the phases were separated by centrifugation at 1000*g* at 4 °C for 10 min in a Beckman Allegra 21R centrifuge. The upper phase enriched in the plasma membrane was diluted by 5-fold in 50 mM Tris-HCl (pH 8.0) and then collected by centrifugation at 45000*g* in a Beckman Optima L-90K ultracentrifuge. The pellet was finally resuspended in 20 mM phosphate buffer (pH 7.4) containing 150 mM NaCl at a protein concentration of 0.2−0.3 mg/mL. The purity of the plasma membrane preparation was assessed from the specific activities of K^+-stimulated, ouabain-inhibited *p*-nitrophenyl phosphatase as a marker for the plasma membrane using an extinction coefficient at 410 nm of 18.8 mM^{-1} cm^{-1} (*21*, *22*), succinate-cytochrome *c* reductase for mitochondria using an extinction coefficient at 600 nm of 19.1 mM^{-1} cm^{-1} (*23*, *24*), and NADPH-cytochrome *c* reductase for the endoplasmic reticulum (ER) using an extinction coefficient at 550 nm of 21.0 mM^{-1} cm^{-1} (*25*, *26*). The plasma membrane preparation was stored at −80 °C for later use.

Removal of Peripheral Membrane Proteins by Sodium Carbonate Treatment. The plasma membrane-enriched fraction was treated with sodium carbonate to remove peripheral membrane proteins (*27*). The plasma membrane preparation (500 μL) was thawed in a 37 °C water bath and then collected by centrifugation at 45000*g* in a Beckman TL-100 ultracentrifuge using a TLA 100.2 rotor (Beckman Coulter). The pellet was resuspended in 200 μL of freshly made 0.1 M Na_2CO_3 and kept on ice for 15 min. The membrane fraction was centrifuged at 52000*g* and 4 °C for 10 min in a Beckman TL-100 ultracentrifuge. The supernatant fraction containing peripheral proteins was removed and the pellet resuspended in 0.1 M Na_2CO_3 to repeat the treatment a second time. The resulting plasma membrane stripped of peripheral proteins was resuspended in 20 mM phosphate buffer (pH 7.4) containing 150 mM NaCl to a protein concentration of 0.2−0.3 mg/mL and stored at −80 °C.

Extraction of Membrane Lipids. Plasma membrane lipids were extracted by the procedure of Folch et al. (*28*). The plasma membrane preparation (500 μL) was collected by centrifugation at 45000*g* in a Beckman TL-100 ultracentrifuge, resuspended in 8 mL of a chloroform/methanol mixture (2:1, v/v), and then mixed at 4 °C overnight. After addition of 1 mL of 1 M H_2SO_4, the sample was vortexed thoroughly and centrifuged at 500*g* for 10 min in a Beckman Allegra 21R centrifuge. The chloroform in the lower phase containing the lipids was transferred to another tube, and a second extraction was performed by addition of 1 mL of 1 M H_2SO_4. Aliquots of the lipids (1 mL) were dried under a stream of N_2 gas, and then further dried in vacuo overnight. The dried plasma membrane lipids were stored at −20 °C.

Preparation of Liposomes. The dried plasma membrane lipids were resuspended in 600 μL of 20 mM phosphate buffer (pH 7.4) containing 150 mM NaCl. Then the lipid suspension was sonicated in a water bath sonicator until the solution became clear. Immediately prior to the binding experiments, liposomes were prepared from the lipid solutions by extrusion through an Avestin polycarbonate filter membrane with a 100 nm pore size using a LiposoFast extruder (Avestin, Ottawa, ON).

Preparation of Synthetic Lipid Liposomes. Synthetic lipid liposomes containing phospholipids, sphingomyelin, and cholesterol were prepared in a similar ratio to that found in the gray matter of the brain (*29*). Stock solutions (2 mM) of dimyristoyl-L-α-phosphatidylcholine (DMPC), dimyristoyl-L-α-phosphatidylserine (DMPS), dimyristoyl-L-α-phosphatidylethanolamine (DMPE), and sphingomyelin (SM) were prepared in a chloroform/methanol mixture (1:1, v/v). A 2 mM stock solution of cholesterol (CL) was prepared in a chloroform/methanol mixture (3:1). DMPC, DMPE, DMPS, SM, and CL were then mixed in a 6:5:2:2:5 ratio (by volume). Aliquots of this mixture (408 μL) were dried under a stream of N_2 gas, and then further dried in vacuo overnight. The dried lipids were stored at −20 °C. Prior to binding assays, liposomes were made from the dried lipids by the same procedure as described above, except for using an Avestin polycarbonate filter membrane with a 50 nm pore size.

TTR Membrane Binding Assay. TTR membrane binding studies employed surface plasmon resonance (SPR) using a Biacore 3000 biosensor equipped with an L1 biosensor chip (Biacore AB, Uppsala, Sweden). In this method, liposomes are immobilized onto the chip via the alkyl groups on the dextran matrix of the chip and incubated to form a lipid bilayer. A solution of TTR was then passed over the lipid bilayer and the amount of binding measured from the change in the SPR signal. Except for experiments which employed different NaCl concentrations, the running buffer was 20 mM phosphate buffer (pH 7.4) containing 150 mM NaCl. The sensor chip was conditioned with 10 μL of 40 mM CHAPS to ensure the surface was free of contaminants. The plasma membrane or the synthetic lipid liposomes (100 μL) were then immobilized onto the chip surface at a flow rate of 2 μL/min, and subsequently, the running buffer was passed over the surface for 10 min after the end of injection to allow for equilibration. NaOH (10 μL of a 10 mM solution) was applied at a rate of 50 μL/min to remove multilamellar lipids. After the chip had been coated with liposomes, an increase of 5000−7000 response units (RU) was obtained, indicating complete coverage of the chip by the lipid bilayer (*29*, *30*). All TTR samples were centrifuged at 13 000 rpm for 1 min with a benchtop centrifuge (Eppendorf 5415 D) prior to the binding assay to remove precipitated proteins. A TTR solution (100 μL) was applied to the membrane bilayer at a rate of 30 μL/min over a period of 200 s, and the association of TTR with the membrane was monitored. TTR was then removed and replaced with the running buffer, and the dissociation of TTR was monitored for a further 10 min. Finally, to remove TTR and regenerate the membrane bilayer for further binding studies without damaging the immobilized membrane bilayer, NaOH (10 μL of a 10 mM solution) was injected at a rate of 50 μL/min. At the end of each assay, 10 μL of 40 mM CHAPS and 2-propanol/50 mM NaOH (4:6, v/v) were injected to strip the membrane bilayer off the sensor chip and regenerate the chip (*31*).

Effect of Ionic Strength on TTR Membrane Binding. To determine the effect of ionic strength on the membrane binding of TTR, after the plasma membrane or the synthetic lipid liposomes had been loaded in 20 mM phosphate buffer (pH 7.4) containing 150 mM NaCl, 20 mM phosphate buffer (pH 7.4) containing 0, 150, or 500 mM NaCl was used as the running buffer. After aging, TTR solutions were buffer exchanged to the corresponding running buffer with Centricon centrifugal filter units with a MW cutoff of 10 000 (Millipore). A TTR concentration of 5 μM was used in this study.

Analysis of Binding Data. The amount of binding was determined from the change in the response units (RU), which is proportional to the mass of the protein bound to the surface of the sensor chip. R_{eq}, the theoretical amount of binding at equilibrium, was calculated using BIAevaluation version 4.1 (Biacore AB) by the formula

$$R_{eq} = \frac{R_{max}}{1 + K_D/C}$$

where R_{eq} is the maximum binding achieved for a given concentration of TTR (C), R_{max} is the theoretical maximum amount of binding calculated from a series of binding curves over a range of TTR concentrations, and K_D is defined as the concentration C required to achieve an R_{eq} of $0.5R_{max}$. Subsequently, the multiple binding curves at different TTR concentrations were used to generate Scatchard plots of the equilibrium binding data (R_{eq}/C vs R_{eq}).

Membrane Fluidity Assay. The effect of TTR amyloid binding on membrane fluidity was assessed by monitoring the fluorescence anisotropy of a membrane-embedded probe, 1,6-diphenyl-1,3,5-hexatriene (DPH). Aged TTR (10 μM) was incubated with 400 μL of the plasma membrane preparation or the synthetic lipid liposomes at 37 °C for 2 h, followed by the addition of DPH (10 μM) and incubation at room temperature for 1 h. Fluorescence anisotropy was measured using a SPEX Fluorolog 1681 0.22m spectrometer (Spex Industries, Edison, NJ) in the L-format with an excitation wavelength of 360 nm and an emission wavelength of 430 nm. Fluorescence anisotropy of DPH was determined over a temperature range of 5−55 °C.

RESULTS

TTR Aggregation. WT TTR and two amyloidogenic TTR mutants (V30M and L55P) were expressed in *E. coli*, and then purified by ammonium sulfate precipitation, ion-exchange chromatography, and size-exclusion chromatography. To examine the ability of TTR proteins to aggregate into amyloid fibrils, WT TTR and the amyloidogenic mutants were incubated (aged) at 37 °C for 1 week, and the time course of aggregation was followed by measuring the turbidity (absorbance) of the solution at 330 nm. WT TTR did not aggregate, as the turbidity of the solution remained constant over time. However, both V30M and L55P TTR rapidly aggregated over the first 48 h of incubation, followed by a slower rate of aggregation between 40 h and 1 week (Figure 1A). The amount of aggregation was greater for L55P TTR than for V30M TTR, consistent with previous reports that L55P TTR is more amyloidogenic than V30M TTR (*32*).

Aggregation was also monitored by size-exclusion chromatography. Little change was seen in the elution profile after WT TTR had been aged for 1 week (Figure 1B). However, aging V30M and L55P TTR resulted in a decrease in the level of tetramers, and the appearance of the high-molecular-mass TTR aggregates (>10^6 Da) and the monomeric TTR (Figure 1B), consistent with previous reports that tetrameric TTR first dissociates into monomers before aggregating into higher-molecular mass amyloid fibrils (*12*). After aging, L55P TTR contained more monomeric and aggregated forms than V30M TTR.

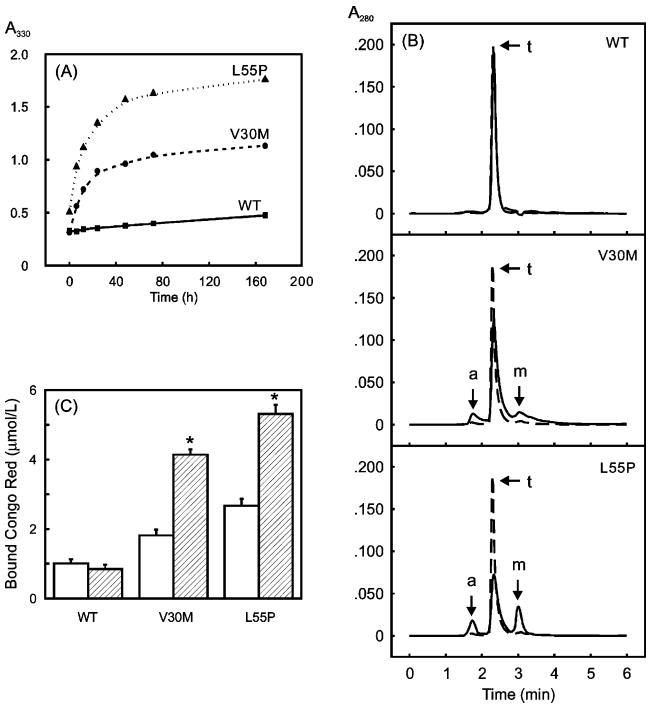

FIGURE 1: Effect of aging on TTR aggregation and amyloid formation. (A) Time course of TTR aggregation as measured by solution turbidity. TTR (40 μM) was aged at 37 °C for 1 week, and the absorbance of the solution was monitored at 330 nm. (B) Analysis of TTR aggregation by size-exclusion HPLC. This panel shows the elution profiles of freshly prepared TTR (40 μM) (dashed line) superimposed with aged TTR after aging for 1 week (solid line). Aggregated TTR (a) with a high molecular mass (>10^6 Da) eluted at 1.8 min. Tetrameric TTR (t) (65 kDa) eluted at 2.3 min, and monomeric TTR (m) (16 kDa) eluted at 3.0 min. (C) TTR amyloid formation as measured by Congo red binding. Freshly prepared TTR solutions (40 μM) (white bars) were compared with aged TTR solutions (cross-hatched bars) after aging for 1 week at 37 °C. Bars show means ± the standard error of the mean (SEM) ($n = 3$). An asterisk indicates a value is significantly different from that of the corresponding incubations using freshly prepared TTR.

Aggregation was also assessed using a Congo red binding assay which measures the concentration of TTR present as amyloid (Figure 1C). Aging the amyloidogenic mutants resulted in a significant increase in the concentration of TTR amyloid, whereas there was no increase in the concentration of TTR amyloid after aging WT TTR. Once again, L55P TTR aggregated more readily than V30M TTR, as the amount of fibrillar TTR was greater for L55P TTR than for V30M TTR.

Cytotoxicity Assays. The cytotoxicity of each type of TTR on SH-SY5Y neuroblastoma cells in culture was investigated using an MTS assay of cell viability. When SH-SY5Y cells were incubated with freshly prepared WT or V30M TTR, there was no significant effect on cell viability (Figure 2A). A 20% decrease in cell viability was detected in the cultures

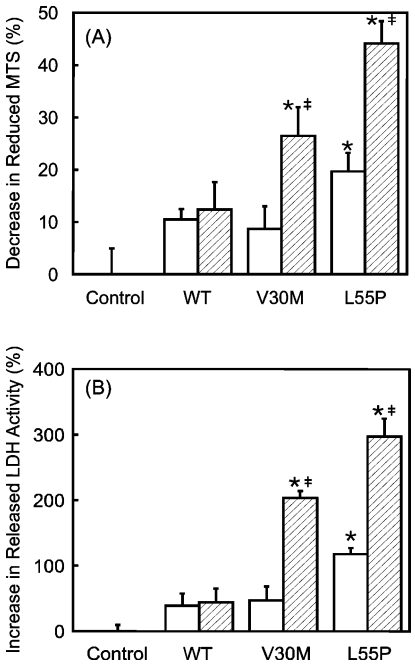

FIGURE 2: Neurotoxicity of TTR on SH-SY5Y cells. (A) Effect of TTR on cell viability measured using an MTS assay. (B) Effect of TTR on cell death measured using an LDH release assay. Freshly prepared (white bars) and aged TTR (cross-hatched bars) (10 μM) was added to culture medium and incubated with the cells at 37 °C for 24 h. The decrease in the level of MTS reduction and the increase in released LDH activity were calculated as a percentage of the respective controls. Bars show means ± SEM ($n = 3$). An asterisk indicates a value is significantly different from those of the controls lacking TTR. A double dagger indicates a significant difference from the corresponding incubation using freshly prepared TTR.

incubated with freshly prepared L55P TTR. Aging increased the cytotoxicity of the amyloidogenic mutants, as there was a 20−30% decrease in cell viability when cells were incubated with aged V30M TTR and a 40−50% decrease in cell viability with aged L55P TTR (Figure 2A). No significant toxic effect was observed when cells were treated with aged WT TTR.

The results of the MTS assay were supported by similar findings obtained using an LDH release assay of cell death. Freshly prepared WT and V30M TTR did not increase the amount of LDH release from the SH-SY5Y cells (Figure 2B). However, when cells were incubated with freshly prepared L55P, there was a 2-fold increase in the amount of LDH release. Aging increased the neurotoxicity of the amyloidogenic mutants, as there was a 3-fold increase in the amount of LDH release when cells were incubated with aged V30M TTR and a 4-fold increase in the amount of LDH release with aged L55P TTR (Figure 2B). The results from the MTS and LDH release assays confirmed that both V30M and L55P TTR are cytotoxic after aging, and that the more amyloidogenic L55P TTR is more toxic than V30M TTR on neuronal cells.

Analysis of Binding of TTR to the Plasma Membrane. To examine the possibility that the cytotoxic effects are due to binding of TTR to the plasma membrane, a plasma membrane-enriched fraction was prepared from SH-SY5Y cells by a two-phase polymer method. This fraction was approximately 4-fold enriched over the total cell lysate in the plasma membrane according to the specific activity of a marker enzyme, *p*-nitrophenylphosphatase [0.76 ± 0.11 vs 0.21 ± 0.04 μmol h^{-1} (mg of protein)$^{-1}$].

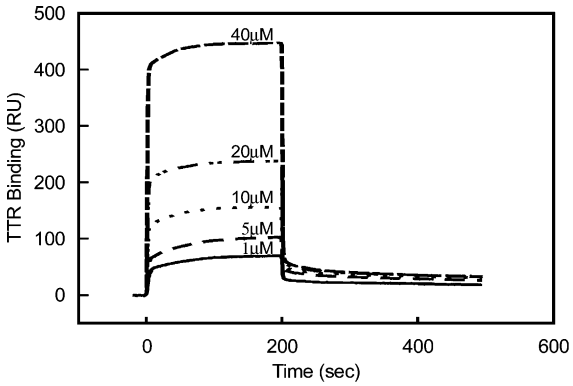

FIGURE 3: Sensorgrams showing reversible binding of TTR to a plasma membrane-enriched preparation. Freshly prepared L55P TTR over a range of concentrations (1−40 μM) was applied over a 200 s time period to the immobilized plasma membrane derived from SH-SY5Y cells. After the termination of TTR application, the membrane was washed with the running buffer to allow for the dissociation of TTR from the membrane.

The binding of TTR to the plasma membrane fraction was then studied using an SPR biosensor. The plasma membrane fraction was applied to an L1 biosensor chip to create an immobilized membrane bilayer. TTR was then applied to the membrane over a range of concentrations (1−40 μM), and binding was observed in real time.

All forms of TTR were found to bind reversibly to the plasma membrane, and the binding was concentration-dependent (Figure 3). Binding rapidly approached equilibrium within 200 s of TTR application, and upon the termination of TTR application, bound TTR rapidly dissociated from the membrane. Only a small residual amount of bound TTR remained after a 20 min wash period.

Scatchard analysis was performed to analyze the binding in more detail. Scatchard plots (R_{eq}/C vs R_{eq}) were nonlinear, suggesting the presence of both high-affinity and low-affinity interactions (Figure 4) (*33*). The equilibrium dissociation constant (K_D) for high-affinity binding of fresh TTR and aged wild-type TTR was 0.5−2.0 μM and for the low-affinity binding was 10−100 μM. The K_D for the high-affinity binding of aged V30M and L55P was 0.1−1.0 μM and for low-affinity binding was 1−10 μM. After WT TTR had been aged for 1 week, the amount of binding was not significantly changed (Figure 4A). However, aging the amyloidogenic mutants resulted in an increase in the amount of TTR binding. The relative order of the amount of binding to the plasma membrane after aging (L55P > V30M > WT TTR) was similar to that of aggregation and cytotoxicity.

Identification of Membrane Binding Constituents. To examine the identity of the membrane components which bind TTR, the plasma membrane was further fractionated. First, peripheral membrane proteins were removed from the plasma membrane by carbonate treatment. The stripped membrane fraction was then applied to an L1 biosensor chip, and the binding of TTR was studied. However, after removal of peripheral proteins from the plasma membrane, the binding of all forms of TTR remained relatively unchanged when compared to that of the intact plasma membrane (Figure 4D−F), indicating that TTR did not bind to a peripheral membrane protein.

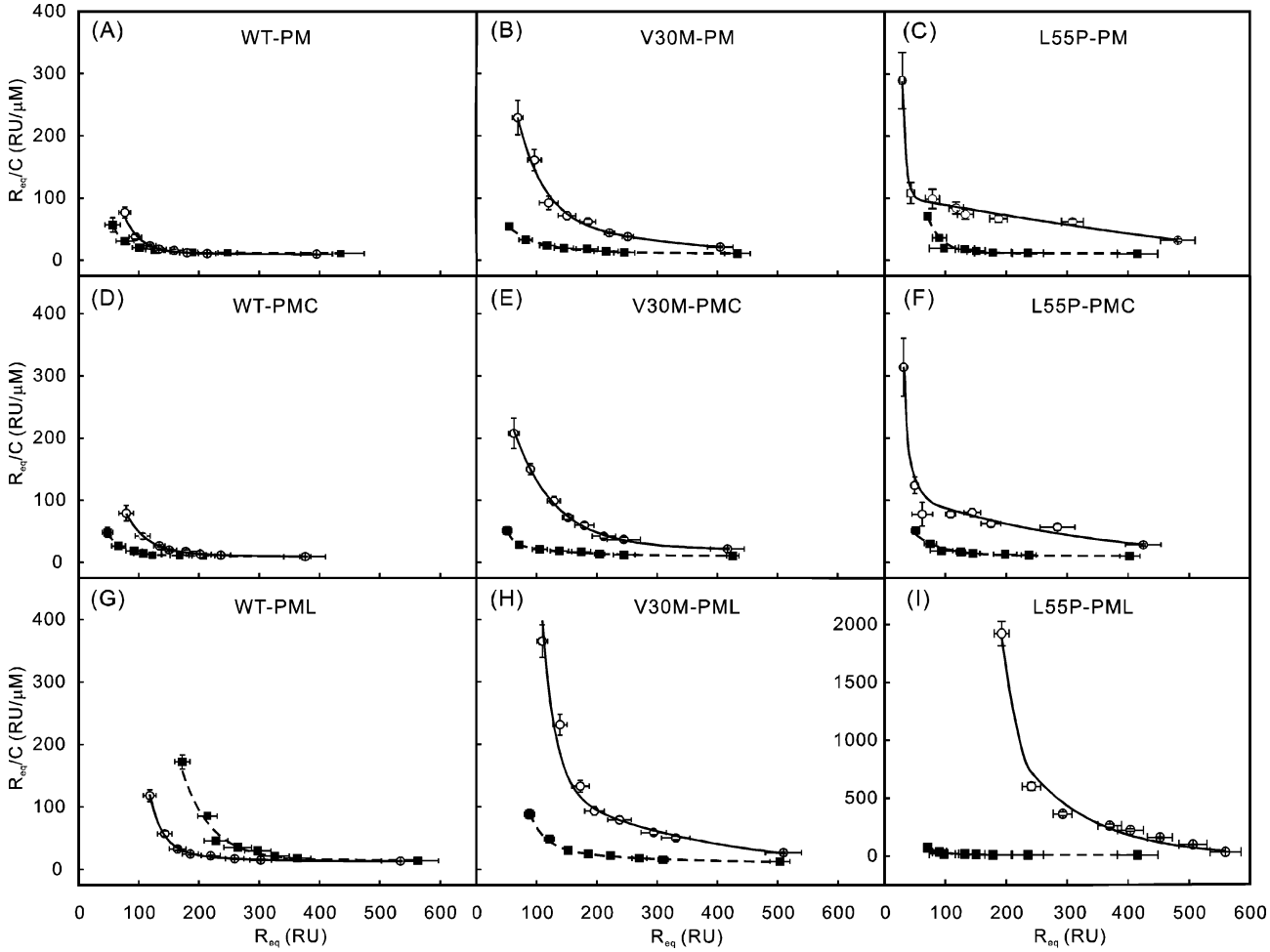

FIGURE 4: Scatchard plots of WT (A, D, and G), V30M (B, E, and H), and L55P (C, F, and I) TTR binding to the intact plasma membrane (PM) (A−C), the plasma membrane treated with carbonate (PMC) (D−F), and the plasma membrane lipid fraction (PML) (G−I). The binding data were obtained over a range of TTR concentrations from 0.1 to 40 μM and then used to calculate the equilibrium binding amount (R_{eq}) (see Experimental Procedures). Values are means ± SEM ($n = 3$). Data for the freshly prepared samples are represented by the filled symbols and the dashed lines, while data for the aged samples are represented by the empty symbols and the solid lines. Panel I has a scale different from that of the other panels.

To examine whether TTR may bind to lipids in the plasma membrane, a lipid fraction was extracted from the membrane by a chloroform/methanol treatment. The membrane-derived lipid extract was then applied to an L1 biosensor chip to form a lipid bilayer, and the binding of TTR was examined. A larger amount of TTR bound to the lipid fraction than to the intact plasma membrane or to the carbonate-treated plasma membrane (Figure 4G−I). The affinity of binding to the lipid fraction, i.e., the slopes of the Scatchard plots, was similar to that of binding to the intact membrane. The effect of aging on TTR binding was also similar. Aging increased the extent of binding of the amyloidogenic mutants, and the amount of binding was higher for aged L55P TTR than for V30M TTR. Therefore, as binding to the membrane-derived lipid extract was similar to that obtained with the intact membrane, it seemed likely that TTR bound principally to a lipid component in the plasma membrane.

To confirm that TTR binds to lipids, synthetic lipid liposomes containing a mixture of phospholipids, sphingomyelin, and cholesterol (DMPC, DMPE, DMPS, SM, and CL in a 6:5:2:2:5 molar ratio) were prepared. The lipid composition was based on the known data of the gray matter of the brain (*34*). The synthetic lipid liposomes were then applied to an L1 biosensor chip to form a bilayer, and the binding of TTR was studied over a range of TTR concentrations (1−40 μM). The binding curves obtained in this manner were compared with those obtained using the plasma membrane.

Like the results obtained from the plasma membrane preparations, TTR bound to the artificial lipid membrane in a complex fashion, resulting in curvilinear Scatchard plots containing both high-affinity and low-affinity interactions (Figure 5). The results with the artificial lipid membrane supported the conclusion that TTR binds principally to lipids. The binding of TTR to the artificial lipid membrane was very similar to the binding obtained with the plasma membrane preparation. As observed previously with the plasma membrane, there was a marked increase in the amount of TTR binding to the artificial lipid membrane after aging for the amyloidogenic mutants, and the same relative order of L55P > V30M > WT TTR was observed in the amount of binding to the artificial lipid membrane (Figure 5).

Effect of Ionic Strength on TTR Membrane Binding. To determine whether the binding of TTR to the plasma membrane was ionic or hydrophobic in character, the effect of ionic strength on TTR binding was examined. TTR binding was assessed at 0, 150, and 500 mM NaCl in the

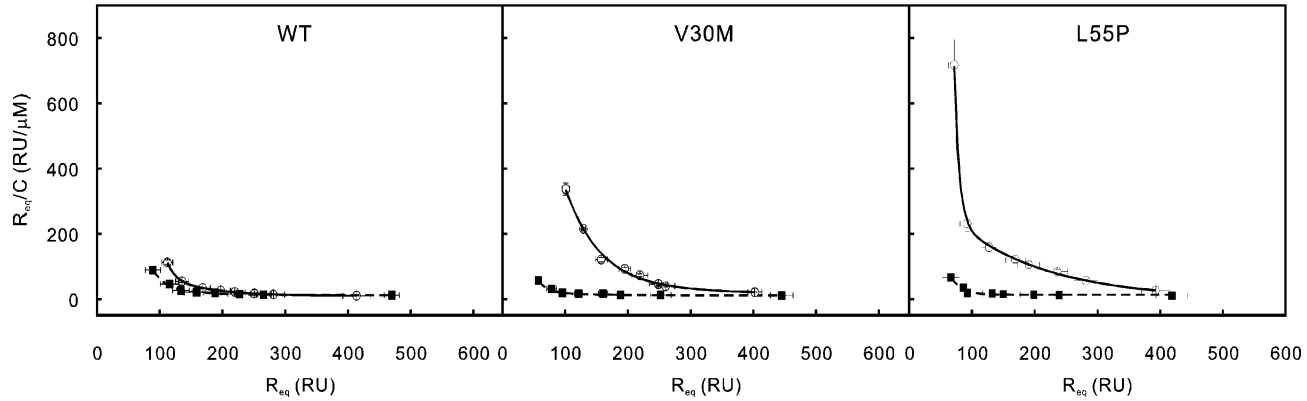

FIGURE 5: Scatchard plots of TTR binding to an artificial lipid membrane containing a mixture of phospholipids, sphingomyelin, and cholesterol. Curves for freshly prepared TTR (filled symbols and dashed lines) and aged TTR (empty symbols and solid lines) are shown. The binding data were collected over a range of TTR concentrations from 0.1 to 40 μM and then used to calculate the equilibrium binding amount (R_{eq}) (see Experimental Procedures). Values are means ± SEM ($n = 3$).

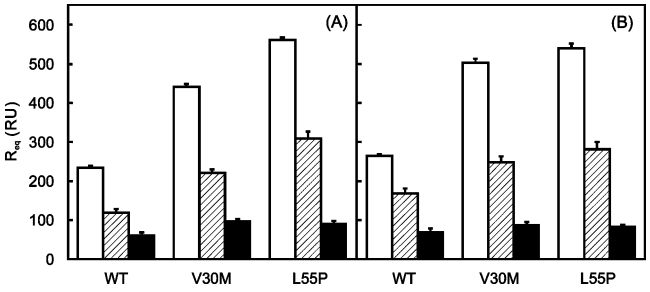

FIGURE 6: Effect of ionic strength on the binding of aged TTR to the plasma membrane (A) and the artificial lipid membrane (B). Aged TTR (5 μM) was applied to the membranes at 0 mM (white bars), 150 mM (cross-hatched bars), and 500 mM NaCl (black bars) in the running buffer. Bars show means ± SEM ($n = 3$). The presence of NaCl significantly inhibited binding in all incubations ($P < 0.001$, ANOVA).

running buffer. The amount of binding (R_{eq}) was determined at different salt concentrations. The amount of TTR binding to the plasma membrane inversely correlated with salt concentration (Figure 6A). A similar relationship between ionic strength and binding was observed with the artificial lipid membrane (Figure 6B), indicating that the binding of TTR to the plasma membrane lipids is predominantly mediated by electrostatic interactions.

Effect of TTR Binding on Membrane Fluidity. A close correlation was observed among TTR aggregation, the amount of membrane binding, and cytotoxicity, suggesting that the binding of aggregated TTR to the plasma membrane may cause cytotoxicity by altering the properties of the membrane. It has been reported that the binding of the amyloid protein of Alzheimer's disease (Aβ) to lipid membranes can change membrane fluidity (*35*, *36*). Therefore, we examined the effect of TTR binding on the fluidity of SH-SY5Y cell plasma membranes and the synthetic lipid liposomes.

To assess membrane fluidity, fluorescence anisotropy of a lipophilic probe (DPH) was examined. DPH fluorescence anisotropy provides a measure of the relative lateral and rotational mobility of molecules in a phospholipid bilayer (*37*). The synthetic lipid liposomes and the plasma membrane were incubated with aged TTR before the addition of DPH, and the fluorescence anisotropy of DPH was measured over the temperature range of 5−55 °C. For the synthetic lipid liposomes, a phase transition temperature (T_m) of 37 °C,

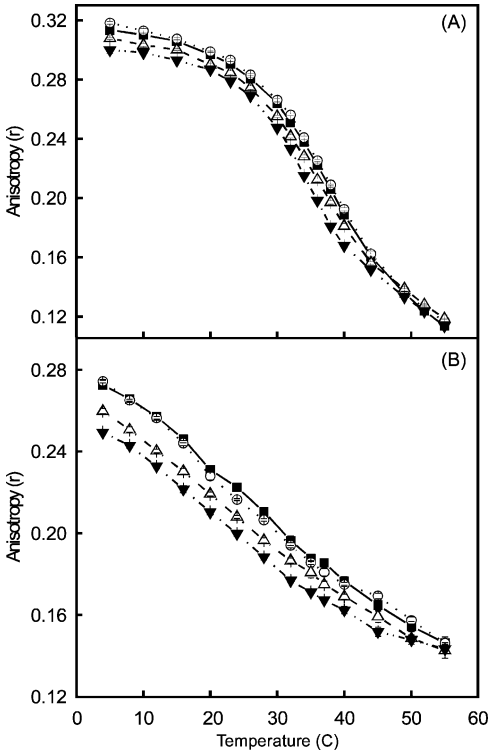

FIGURE 7: Effect of aged TTR (10 μM) on the fluidity of the synthetic lipid liposomes (A) and the plasma membrane preparation (B). Incubations without TTR (■) and with WT (○), V30M (△), and L55P (▼) TTR are shown. The membrane fluidity was estimated from the fluorescence anisotropy of DPH. Values are means ± SEM ($n = 10$).

calculated from the point of inflection of the curve (*38*), was observed (Figure 7A). No apparent T_m was observed with the plasma membrane (Figure 7B). Incubation with aged WT TTR did not significantly alter the DPH fluorescence anisotropy of either the synthetic lipid liposomes or the plasma membrane. However, at 37 °C, incubation with aged V30M decreased the DPH anisotropy of the synthetic lipid liposomes and the plasma membrane by 4% ($P < 0.01$) and 6% ($P < 0.01$), respectively, while aged L55P TTR decreased the DPH anisotropy of the synthetic lipid liposomes and the plasma membrane by 12% ($P < 0.01$) and 10% ($P < 0.01$), respectively, indicating increased membrane fluidity in all cases. The effect was seen at temperatures up to 45−50 °C, where the fluorescence anisotropy curves

started to merge. Consistent with the results of cytotoxicity and membrane binding, the relative order of effect on membrane fluidity was as follows: L55P > V30M > WT TTR ≅ control (no TTR).

DISCUSSION

While previous studies (*32*) have shown that the neurotoxicity of TTR is correlated with its amyloidogenicity, the mechanism by which TTR exerts cytotoxic effects has not been examined in detail. This study demonstrates, for the first time, that TTR can bind electrostatically to lipids of the plasma membrane. The amount of TTR membrane binding correlated closely with the degree of neurotoxicity generated in cell culture, indicating that binding of TTR to the plasma membrane is an important step in the induction of TTR neurotoxicity. Binding of TTR to the plasma membrane also increased the membrane fluidity. As membrane fluidity is known to be important for normal cell function and viability (*39*), we suggest that interaction of TTR with the plasma membrane may alter the dynamic properties of the plasma membrane, thereby causing a decrease in cell viability.

After aging, the amount of binding to the plasma membrane was higher for the amyloidogenic TTR mutants than for WT TTR. The relative order of the amount of binding to the plasma membrane, cytotoxicity, and aggregation was as follows in each case: L55P > V30M > WT TTR. The observation that membrane binding correlated with cytotoxicity and aggregation is consistent with early reports. For example, we recently showed that the binding of Aβ to lipid membranes and the cytotoxicity of Aβ were correlated (*17*). Similarly, conversion of the native nontoxic form of the prion protein (PrP^{C}) to the toxic amyloid form (PrP^{Sc}) causes a 10-fold increase in the amount of membrane binding (*40*). Thus, although amyloidogenic proteins have little similarity in their primary sequences, they may all share a common mechanism by which they induce cytotoxicity, i.e., by binding to the plasma membrane.

Although putative membrane receptors for TTR have been reported (*41*−*43*), prior to this study, the identity of the components within the plasma membrane that bind TTR had not been determined. Our data clearly indicate that TTR principally binds to lipids in the plasma membrane. This conclusion is supported by the finding that removal of peripheral membrane proteins by carbonate treatment did not alter the membrane binding of TTR, and that removal of all membrane proteins, including integral proteins, resulted in an increase in the amount of TTR binding. Moreover, the binding of TTR to an artificial lipid membrane was very similar to that of the plasma membrane preparation.

Membrane binding of TTR inversely correlated with ionic strength, supporting the view that TTR binds to the plasma membrane predominantly through electrostatic interactions. Electrostatic interactions may also mediate the membrane binding of Aβ and prion proteins (PrP) (*17*, *40*). TTR probably binds to the polar region of phospholipid headgroups on the surface of the plasma membrane. However, it is not clear which lipid species are involved in TTR binding.

The membrane binding of TTR was composed of multiple components, and both high-affinity and low-affinity interactions were observed. The complex nature of TTR binding was probably due to the heterogeneous composition of the TTR preparations, because after aging, TTR forms a mixture of tetramers, monomers, and high-molecular mass aggregates. As aging increased the proportion of aggregates in the amyloidogenic TTR mutants, the difference in binding affinity after aging seen for the mutants is likely to be the consequence of an increased level of aggregation. Each of the TTR aggregates may bind with different affinity to the plasma membrane, making it difficult to define the exact affinity. Nonetheless, the equilibrium dissociation constants were in the micromolar range, the same magnitude as the physiological concentration of TTR (*4*).

Binding of TTR to the plasma membrane also caused an increase in membrane fluidity. This increase in membrane fluidity with binding may be an important step in the induction of TTR neurotoxicity. Alterations in membrane fluidity have also been reported for Aβ, although there are conflicting data. $A\beta_{1-40}$ has been reported to increase neuronal membrane fluidity (*36*), but a decrease in membrane fluidity has been reported for artificial lipid membranes (*44*). In addition, binding of PrP decreases the membrane fluidity of neuroblastoma cells (*45*). It is now well established that membrane fluidity plays a crucial role in the regulation of cell function (*46*, *47*). Changes in membrane fluidity can affect the activity of a variety of membrane proteins that are vital for cell viability. Regions of low fluidity containing high concentrations of cholesterol and sphingolipids as well as specialized membrane receptors have been found on the surface of membranes (*39*). These regions (i.e., lipid rafts) are important for membrane receptor clustering and signal transduction through intracellular mediators such as the Rho GTPase which regulates cytoskeletal morphology (*48*). Other studies have suggested that lipid rafts may be involved in Aβ production and the induction of the cytotoxicity of Aβ (*49*, *50*). Since alterations in the membrane microenvironment via changes in membrane fluidity can have profound effects on cell function and viability (*39*), it is possible that TTR binding disrupts lipid raft-mediated cell signaling.

In FAP, extracellular TTR amyloid deposits are located in the endoneurium, invariably accompanied by axonal degeneration and disrupture of neuronal cell morphology (*5*, *14*). So far, the only treatment available for FAP is liver transplantation to stop further production of misfolded TTR (*51*). However, after liver transplantation, mutant TTR synthesized in the choroid plexus will continue being secreted into the cerebrospinal fluid, and subsequently cause dementia (*4*). This study provides further evidence for the mechanism of neurotoxicity caused by TTR amyloid. Elucidation of the downstream events associated with TTR membrane binding may eventually lead to the identification of new targets for drug development. Furthermore, as the mechanism of cytotoxicity may be similar for different amyloidoses, this study also sheds light on the mechanism of pathogenesis of other amyloidoses.

ACKNOWLEDGMENT

We thank Dr. Andrew H. Clayton (Ludwig Institute of Cancer Research, Melbourne, Australia) for assistance with the fluorescence anisotropy experiments.

REFERENCES

1. Agorogiannis, E. I., Agorogiannis, G. I., Papadimitriou, A., and Hadjigeorgiou, G. M. (2004) Protein misfolding in neurodegenerative diseases, *Neuropathol. Appl. Neurobiol. 30*, 215−224.
2. Chaney, M. O., Baudry, J., Esh, C., Childress, J., Luehrs, D. C., Kokjohn, T. A., and Roher, A. E. (2003) Aβ, aging, and Alzheimer's disease: A tale, models, and hypotheses, *Neurol. Res. 25*, 581−589.
3. Small, D. H., Mok, S. S., and Bornstein, J. C. (2001) Alzheimer's disease and Aβ toxicity: Drom top to bottom, *Nat. Rev. Neurosci. 2*, 595−598.
4. Schreiber, G., and Richardson, S. J. (1997) The evolution of gene expression, structure and function of transthyretin, *Comp. Biochem. Physiol., Part B: Biochem. Mol. Biol. 116*, 137−160.
5. Saraiva, M. J. (2003) Cellular consequences of transthyretin deposition, *Amyloid 10* (Suppl. 1), 13−16.
6. Benson, M. D. (1989) Familial amyloidotic polyneuropathy, *Trends Neurosci. 12*, 88−92.
7. Murakami, T., Uchino, M., and Ando, M. (1995) Genetic abnormalities and pathogenesis of familial amyloidotic polyneuropathy, *Pathol. Int. 45*, 1−9.
8. Hamilton, J. A., Steinrauf, L. K., Braden, B. C., Liepnieks, J., Benson, M. D., Holmgren, G., Sandgren, O., and Steen, L. (1993) The X-ray crystal structure refinements of normal human transthyretin and the amyloidogenic Val-30→Met variant to 1.7-Å resolution, *J. Biol. Chem. 268*, 2416−2424.
9. Selkoe, D. J. (2003) Folding proteins in fatal ways, *Nature 426*, 900−904.
10. Eneqvist, T., and Sauer-Eriksson, A. E. (2001) Structural distribution of mutations associated with familial amyloidotic polyneuropathy in human transthyretin, *Amyloid 8*, 149−168.
11. Colon, W., Lai, Z., McCutchen, S. L., Miroy, G. J., Strang, C., and Kelly, J. W. (1996) FAP mutations destabilize transthyretin facilitating conformational changes required for amyloid formation, *Ciba Found. Symp. 199*, 228−242.
12. Cardoso, I., Goldsbury, C. S., Muller, S. A., Olivieri, V., Wirtz, S., Damas, A. M., Aebi, U., and Saraiva, M. J. (2002) Transthyretin fibrillogenesis entails the assembly of monomers: A molecular model for in vitro assembled transthyretin amyloid-like fibrils, *J. Mol. Biol. 317*, 683−695.
13. Olofsson, A., Ostman, J., and Lundgren, E. (2002) Amyloid: Morphology and toxicity, *Clin. Chem. Lab. Med. 40*, 1266−1270.
14. Said, G. (2003) Familial amyloid polyneuropathy: Mechanisms leading to nerve degeneration, *Amyloid 10* (Suppl. 1), 7−12.
15. Yip, C. M., Darabie, A. A., and McLaurin, J. (2002) Aβ42-peptide assembly on lipid bilayers, *J. Mol. Biol. 318*, 97−107.
16. Kakio, A., Nishimoto, S. I., Yanagisawa, K., Kozutsumi, Y., and Matsuzaki, K. (2001) Cholesterol-dependent formation of GM1 ganglioside-bound amyloid β-protein, an endogenous seed for Alzheimer amyloid, *J. Biol. Chem. 276*, 24985−24990.
17. Subasinghe, S., Unabia, S., Barrow, C. J., Mok, S. S., Aguilar, M. I., and Small, D. H. (2003) Cholesterol is necessary both for the toxic effect of Aβ peptides on vascular smooth muscle cells and for Aβ binding to vascular smooth muscle cell membranes, *J. Neurochem. 84*, 471−479.
18. Aguilar, M. I., and Small, D. H. (2004) Surface plasmon resonance for the analysis of β-amyloid interactions and fibril formation in Alzheimer's disease research, *Neurotox. Res. 7*, 17−27.
19. Lai, Z., Colon, W., and Kelly, J. W. (1996) The acid-mediated denaturation pathway of transthyretin yields a conformational intermediate that can self-assemble into amyloid, *Biochemistry 35*, 6470−6482.
20. Morre, D. J., and Morre, D. M. (1989) Preparation of mammalian plasma membranes by aqueous two-phase partition, *BioTechniques 7*, 946−956.
21. Vaillant, F., Larm, J. A., McMullen, G. L., Wolvetang, E. J., and Lawen, A. (1996) Effectors of the mammalian plasma membrane NADH-oxidoreductase system. Short-chain ubiquinone analogues as potent stimulators, *J. Bioenerg. Biomembr. 28*, 531−540.
22. Coimbra, E. S., Goncalves-da-Costa, S. C., Corte-Real, S., De Freitas, F. G., Durao, A. C., Souza, C. S., Silva-Santos, M. I., and Vasconcelos, E. G. (2002) Characterization and cytochemical localization of an ATP diphosphohydrolase from *Leishmania amazonensis promastigotes*, *Parasitology 124*, 137−143.
23. Morre, D. M., and Morre, D. J. (2000) Aqueous two-phase partition applied to the isolation of plasma membranes and Golgi apparatus from cultured mammalian cells, *J. Chromatogr., B: Biomed. Sci. Appl. 743*, 377−387.
24. Padilla, S., Jonassen, T., Jimenez-Hidalgo, M. A., Fernandez-Ayala, D. J., Lopez-Lluch, G., Marbois, B., Navas, P., Clarke, C. F., and Santos-Ocana, C. (2004) Demethoxy-Q, an intermediate of coenzyme Q biosynthesis, fails to support respiration in *Saccharomyces cerevisiae* and lacks antioxidant activity, *J. Biol. Chem. 279*, 25995−26004.
25. Sottocasa, G. L., Kuylenstierna, B., Ernster, L., and Bergstrand, A. (1967) An electron-transport system associated with the outer membrane of liver mitochondria. A biochemical and morphological study, *J. Cell Biol. 32*, 415−438.
26. Dimova, S., Hoet, P. H., and Nemery, B. (2001) Xenobiotic-metabolizing enzyme activities in primary cultures of rat type II pneumocytes and alveolar macrophages, *Drug Metab. Dispos. 29*, 1349−1354.
27. Fujiki, Y., Hubbard, A. L., Fowler, S., and Lazarow, P. B. (1982) Isolation of intracellular membranes by means of sodium carbonate treatment: Application to endoplasmic reticulum, *J. Cell Biol. 93*, 97−102.
28. Folch, J., Lees, M., and Sloane Stanley, G. H. (1957) A simple method for the isolation and purification of total lipides from animal tissues, *J. Biol. Chem. 226*, 497−509.
29. Erb, E. M., Chen, X., Allen, S., Roberts, C. J., Tendler, S. J., Davies, M. C., and Forsen, S. (2000) Characterization of the surfaces generated by liposome binding to the modified dextran matrix of a surface plasmon resonance sensor chip, *Anal. Biochem. 280*, 29−35.
30. Cooper, M. A., Try, A. C., Carroll, J., Ellar, D. J., and Williams, D. H. (1998) Surface plasmon resonance analysis at a supported lipid monolayer, *Biochim. Biophys. Acta 1373*, 101−111.
31. Abdiche, Y. N., and Myszka, D. G. (2004) Probing the mechanism of drug/lipid membrane interactions using Biacore, *Anal. Biochem. 328*, 233−243.
32. Quintas, A., Saraiva, M. J., and Brito, R. M. (1997) The amyloidogenic potential of transthyretin variants correlates with their tendency to aggregate in solution, *FEBS Lett. 418*, 297−300.
33. Dahlquist, F. W. (1978) The meaning of Scatchard and Hill plots, *Methods Enzymol. 48*, 270−299.
34. Suzuki, K. (1976) in *Basic Neurochemistry* (Siegel, G. J., Albers, R. W., Katzman, R., and Agranoff, B. W., Eds.) pp 308−328, Little, Brown and Co., Boston.
35. Muller, W. E., Koch, S., Eckert, A., Hartmann, H., and Scheuer, K. (1995) β-Amyloid peptide decreases membrane fluidity, *Brain Res. 674*, 133−136.
36. Chochina, S. V., Avdulov, N. A., Igbavboa, U., Cleary, J. P., O'Hare, E. O., and Wood, W. G. (2001) Amyloid β-peptide1−40 increases neuronal membrane fluidity: Role of cholesterol and brain region, *J. Lipid Res. 42*, 1292−1297.
37. Kao, Y. L., Chong, P. L., and Huang, C. H. (1990) Dynamic motions of 1,6-diphenyl-1,3,5-hexatriene in interdigitated C(18): C(10)phosphatidylcholine bilayers, *Biophys. J. 58*, 947−956.
38. Lentz, B. R., Barenholz, Y., and Thompson, T. E. (1976) Fluorescence depolarization studies of phase transitions and fluidity in phospholipid bilayers. 2 Two-component phosphatidylcholine liposomes, *Biochemistry 15*, 4529−4537.
39. Simons, K., and Toomre, D. (2000) Lipid rafts and signal transduction, *Nat. Rev. Mol. Cell Biol. 1*, 31−39.
40. Rymer, D. L., and Good, T. A. (2000) The role of prion peptide structure and aggregation in toxicity and membrane binding, *J. Neurochem. 75*, 2536−2545.
41. Sousa, M. M., and Saraiva, M. J. (2001) Internalization of transthyretin. Evidence of a novel yet unidentified receptor-associated protein (RAP)-sensitive receptor, *J. Biol. Chem. 276*, 14420−14425.
42. Kuchler-Bopp, S., Dietrich, J. B., Zaepfel, M., and Delaunoy, J. P. (2000) Receptor-mediated endocytosis of transthyretin by ependymoma cells, *Brain Res. 870*, 185−194.
43. Sousa, M. M., Yan, S. D., Stern, D., and Saraiva, M. J. (2000) Interaction of the receptor for advanced glycation end products (RAGE) with transthyretin triggers nuclear transcription factor kB (NF-kB) activation, *Lab. Invest. 80*, 1101−1110.
44. Xiaocui, M., Sha, Y., Lin, K., and Nie, S. (2002) The effect of fibrillar Aβ1−40 on membrane fluidity and permeability, *Protein Pept. Lett. 9*, 173−178.
45. Wong, K., Qiu, Y., Hyun, W., Nixon, R., VanCleff, J., Sanchez-Salazar, J., Prusiner, S. B., and DeArmond, S. J. (1996) Decreased receptor-mediated calcium response in prion-infected cells correlates with decreased membrane fluidity and IP3 release, *Neurology 47*, 741−750.

46. Gimpl, G., Burger, K., and Fahrenholz, F. (1997) Cholesterol as modulator of receptor function, *Biochemistry 36*, 10959−10974.
47. Miyamoto, A., Araiso, T., Koyama, T., and Ohshika, H. (1990) Membrane viscosity correlates with α1-adrenergic signal transduction of the aged rat cerebral cortex, *J. Neurochem. 55*, 70−75.
48. Fessler, M. B., Arndt, P. G., Frasch, S. C., Lieber, J. G., Johnson, C. A., Murphy, R. C., Nick, J. A., Bratton, D. L., Malcolm, K. C., and Worthen, G. S. (2004) Lipid rafts regulate lipopolysaccharide-induced activation of Cdc42 and inflammatory functions of the human neutrophil, *J. Biol. Chem. 279*, 39989−39998.
49. Stuermer, C. A., Langhorst, M. F., Wiechers, M. F., Legler, D. F., Von Hanwehr, S. H., Guse, A. H., and Plattner, H. (2004) PrPc capping in T cells promotes its association with the lipid raft proteins reggie-1 and reggie-2 and leads to signal transduction, *FASEB J. 18*, 1731−1733.
50. Kawarabayashi, T., Shoji, M., Younkin, L. H., Wen-Lang, L., Dickson, D. W., Murakami, T., Matsubara, E., Abe, K., Ashe, K. H., and Younkin, S. G. (2004) Dimeric amyloid β protein rapidly accumulates in lipid rafts followed by apolipoprotein E and phosphorylated τ accumulation in the Tg2576 mouse model of Alzheimer's disease, *J. Neurosci. 24*, 3801−3809.
51. Skinner, M., Lewis, W. D., Jones, L. A., Kasirsky, J., Kane, K., Ju, S. T., Jenkins, R., Falk, R. H., Simms, R. W., and Cohen, A. S. (1994) Liver transplantation as a treatment for familial amyloidotic polyneuropathy, *Ann. Intern. Med. 120*, 133−134.

BI050700M